21. M. Jutzi, E. Asphaug, *Nature* **476**, 69 (2011).
22. A. Harris, in R. Greenberg, A. Brahic, Eds., *Planetary Rings* (Univ. of Arizona Press, Tucson, 1984), pp. 641–659.
23. S. Charnoz, A. Morbidelli, L. Dones, J. Salmon, *Icarus* **199**, 413 (2009).
24. R. M. Canup, *Nature* **468**, 943 (2010).
25. L. Dones, *Icarus* **92**, 194 (1991).
26. A. Morbidelli, K. Tsiganis, K. Batygin, A. Crida, R. Gomes, *Icarus* **219**, 737 (2012).
27. L. W. Esposito, J. E. Colwell, *Nature* **339**, 605 (1989).
28. D. P. Rubincam, *Icarus* **184**, 532 (2006).

Acknowledgments: This work was partially funded by the French Programme National de Planétologie. S. Charnoz was supported by a "Labex UnivEarths" grant of Univ. Paris Diderot, Paris Sorbonne Cité, and by CEA-SAp. We thank A. Morbidelli, D. Nesvorny, and N. Murdoch for comments and help in the writing of this manuscript.

Supplementary Materials
www.sciencemag.org/cgi/content/full/338/6111/1196/DC1
Supplementary Text
Figs. S1 and S2
References (*29*–*39*)

22 June 2012; accepted 12 October 2012
10.1126/science.1226477

Chemically and Geographically Distinct Solid-Phase Iron Pools in the Southern Ocean

B. P. von der Heyden,[1,2] A. N. Roychoudhury,[1]* T. N. Mtshali,[1,3] T. Tyliszczak,[4] S. C. B. Myneni[2]

Iron is a limiting nutrient in many parts of the oceans, including the unproductive regions of the Southern Ocean. Although the dominant fraction of the marine iron pool occurs in the form of solid-phase particles, its chemical speciation and mineralogy are challenging to characterize on a regional scale. We describe a diverse array of iron particles, ranging from 20 to 700 nanometers in diameter, in the waters of the Southern Ocean euphotic zone. Distinct variations in the oxidation state and composition of these iron particles exist between the coasts of South Africa and Antarctica, with different iron pools occurring in different frontal zones. These speciation variations can result in solubility differences that may affect the production of bioavailable dissolved iron.

Dissolved, or soluble, iron plays a central role in vital phytoplankton cellular processes, including photosynthesis and the coupled uptake of CO_2 in oceans (*1*, *2*). The concentration of soluble Fe is strongly linked to ocean primary productivity. However, the solubility of Fe is low in oxygenated seawater; the majority of Fe in oceans exists in the form of nanoparticles (<0.2 μm) and biogenic and lithogenic colloids (>0.2 μm). This particulate-bound Fe constitutes as much as 65 to 85% of the total dissolvable Fe fraction in the mixed layer of the Southern Ocean (*3*–*5*). Considering the magnitude of this particulate-bound Fe pool, which is an important reserve source of Fe for photosynthetic organisms, the observation of Fe limitation in certain parts of the Southern Ocean is surprising.

Both the solubility and the bioavailability of particulate-bound Fe vary according to differences in Fe oxidation state, mineralogy, crystallinity, structural impurities (e.g., Al), and the structure and concentration of dissolved organic ligands (*6*–*8*). To improve our understanding of Fe limitation in the Southern Ocean, we examined the structure and chemistry of Fe particles from water samples collected on three different scientific cruises: South African National Antarctic Expedition (SANAE) 49, SANAE 50, and GEOTRACES D357 (*5*). This strategy ensured samples across the fronts of the Southern Ocean, which distinguish water masses with different hydrographic characteristics. The distribution of Fe in particles as a function of particle size was analyzed by collecting high-resolution Fe maps (resolution ~12 nm) at the Fe L_3-absorption edge (~710 eV) (Fig. 1). The oxidation state and coordination environment of Fe in particles were analyzed by collecting Fe L_3-edge x-ray absorption near-edge structure (XANES) spectra. We also measured the association of Fe with Al, a solubility modifier and source indicator. The distribution and chemistry of Al was similarly analyzed using Al maps and XANES spectra at the Al K-edge (~1570 eV).

[1]Department of Earth Sciences, Stellenbosch University, Private Bag X1, Matieland 7602, South Africa. [2]Department of Geosciences, Princeton University, Princeton, NJ 08544, USA. [3]CSIR, P.O. Box 320, Stellenbosch 7600, South Africa. [4]Advanced Light Source, Lawrence Berkeley National Laboratory, University of California, Berkeley, CA 94720, USA.

*To whom correspondence should be addressed. E-mail: roy@sun.ac.za

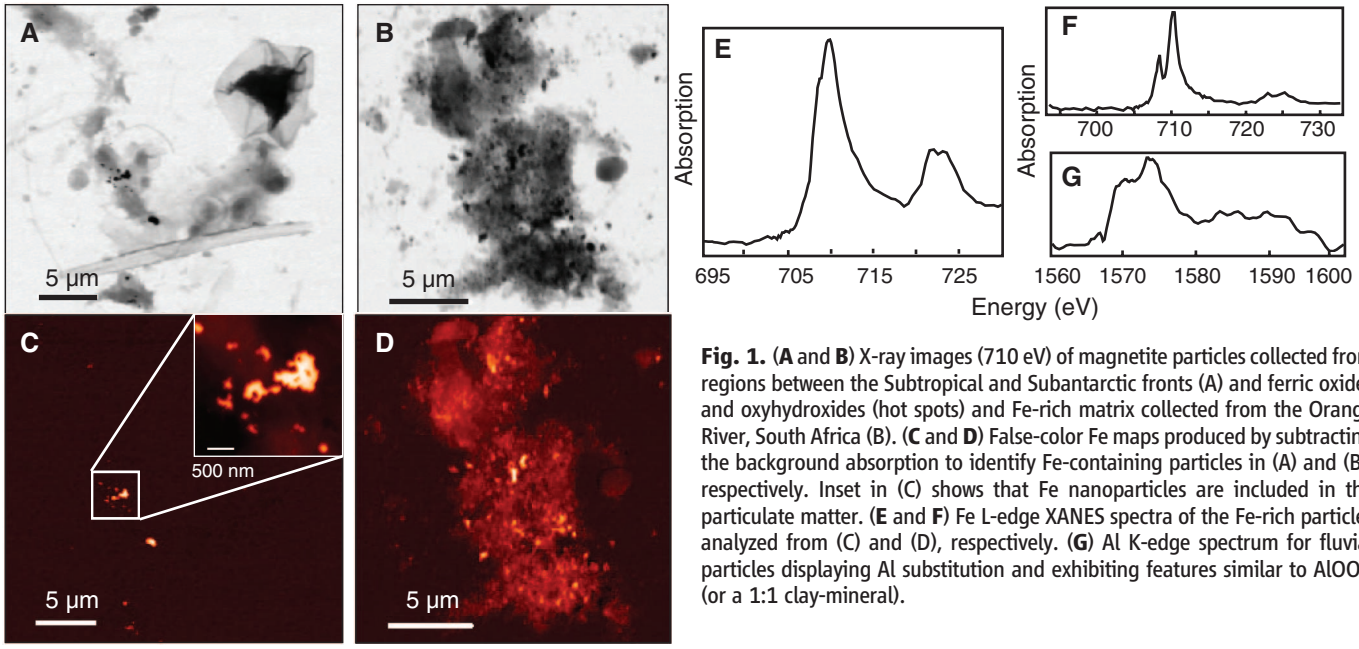

Fig. 1. (**A** and **B**) X-ray images (710 eV) of magnetite particles collected from regions between the Subtropical and Subantarctic fronts (A) and ferric oxides and oxyhydroxides (hot spots) and Fe-rich matrix collected from the Orange River, South Africa (B). (**C** and **D**) False-color Fe maps produced by subtracting the background absorption to identify Fe-containing particles in (A) and (B), respectively. Inset in (C) shows that Fe nanoparticles are included in the particulate matter. (**E** and **F**) Fe L-edge XANES spectra of the Fe-rich particles analyzed from (C) and (D), respectively. (**G**) Al K-edge spectrum for fluvial particles displaying Al substitution and exhibiting features similar to AlOOH (or a 1:1 clay-mineral).

All samples were analyzed at the Advanced Light Source x-ray spectromicroscopy facility, which allows collection of images and XANES spectra at a resolution of 12 nm under ambient conditions (*9*).

The Fe L_3-edge XANES spectra are sensitive to the oxidation state and the coordination environment of Fe (*10*, *11*). Specifically, the energy differences (ΔeV) between the two main transitions and their intensity ratios can be used to distinguish Fe(II) phases from Fe(III) phases and to discern variations in the coordination environment for each oxidation state (Fig. 2). On the basis of their ΔeV and intensity ratio values in the L_3 edge, we categorize the Fe-rich phases into five distinct chemical classes: pure Fe(III) species (including oxyhydroxides; purity refers to valence state and not speciation), pure Fe(II) species, magnetite, and two mixed-valence phases that show a more varied distribution on the spectral plot (Fig. 2). Although constituent mineral phases in Fe particles can be identified using the Fe L_3-edge spectra (fig. S1), we have limited our classification to these five broad classes because mineral identification in natural samples is complicated by the presence of chemical impurities, surface coatings, and poor crystallinity.

The Fe maps of particulate matter from the Southern Ocean are largely characterized by single isolated particles; where present, the surrounding organic and mineral matrix is conspicuously poor in Fe (Fig. 1, A and C). The discrete particles are 20 to 700 nm in diameter, with a mean size of ~200 nm. Larger particles, exceeding sizes of 500 nm, are much less common and are uniquely confined to sites near continental and island shelves. Although an apparent correlation between the size of particles and their Fe valence state and coordination environment was absent, the pure Fe(II) phases are generally larger and have spectral features indicative of greater variability in their Fe coordination environment. The chemistry of mixed-valence phases is not uniform, and their spectra do not correlate to those of known Fe minerals (fig. S1). This suggests the presence of mineral mixtures and structural heterogeneity, possibly caused by the presence of Fe(II) and Fe(III) amorphous phases and/or binding to inorganic and organic ligands. In contrast to the discrete nature and sparse distribution of these marine particles, fluvial Fe-rich particles in streams draining into the South Atlantic Ocean (Orange, Olifants, and Berg rivers) are much more abundant, larger (20 nm to 5 μm), and are commonly associated with Fe-rich inorganic and organic matrices (Fig. 1, B and D).

Iron associated with solid phases displayed speciation variation along the two transects sampled—one between SANAE (coast of Queen Maud Land, Antarctica) and Cape Town, the other between SANAE and South Georgia Island (Fig. 3). Samples from north of the Subtropical Front (i.e., those most proximal to the African continent) show the largest degree of chemical heterogeneity, consisting of predominantly Fe(III)-rich particles with substantial Al association. The water mass between the Subtropical and Subantarctic fronts, which receives relatively high atmospheric dust inputs from Patagonia (*12*), is overwhelmingly dominated by magnetite. Between the Subantarctic Front and the Southern Boundary where deep circumpolar waters upwell (*13*, *14*), Fe particles predominantly contain Fe(III) phases. The Fe(III) phases in these frontal zones display x-ray spectral features more characteristic of Fe(III) oxyhydroxides than Fe(III) oxides (Fig. 2 and fig. S1). In contrast, samples from south of the Southern Boundary, in the Weddell Sea gyre, are largely composed of particles rich in Fe(II). Such a high abundance of Fe(II)-rich particles and magnetite in the oxygen-rich photic zone is surprising,

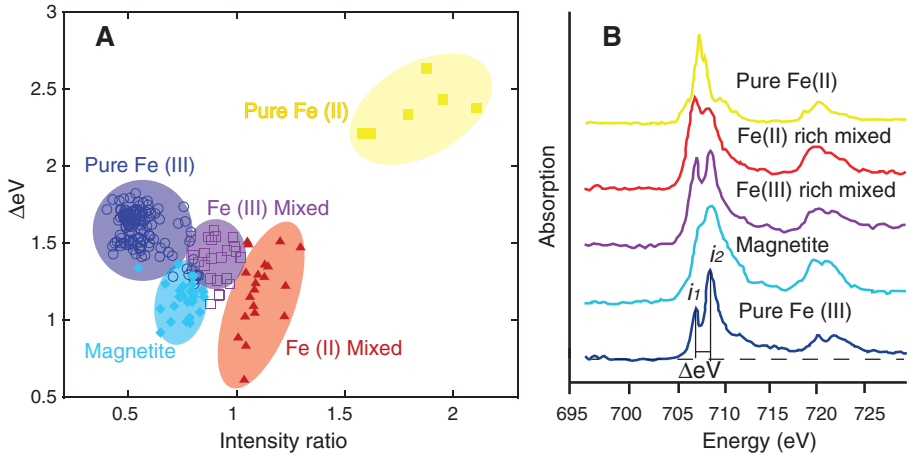

Fig. 2. (**A**) Iron particle speciation plotted and defined according to the particles' spectral features. Pure Fe(III), pure Fe(II), and magnetite phases occupy discrete fields; the mixed-valence species are distinguished by their variations in spectral intensity ratios. (**B**) Generalized Fe L-edge XANES spectra of the five species identified in the South Atlantic and Southern oceans; colors correspond to fields in (A). The ΔeV value is calculated as the energy difference between peaks i_1 and i_2; the intensity ratio value is given as absorption intensity i_1/i_2.

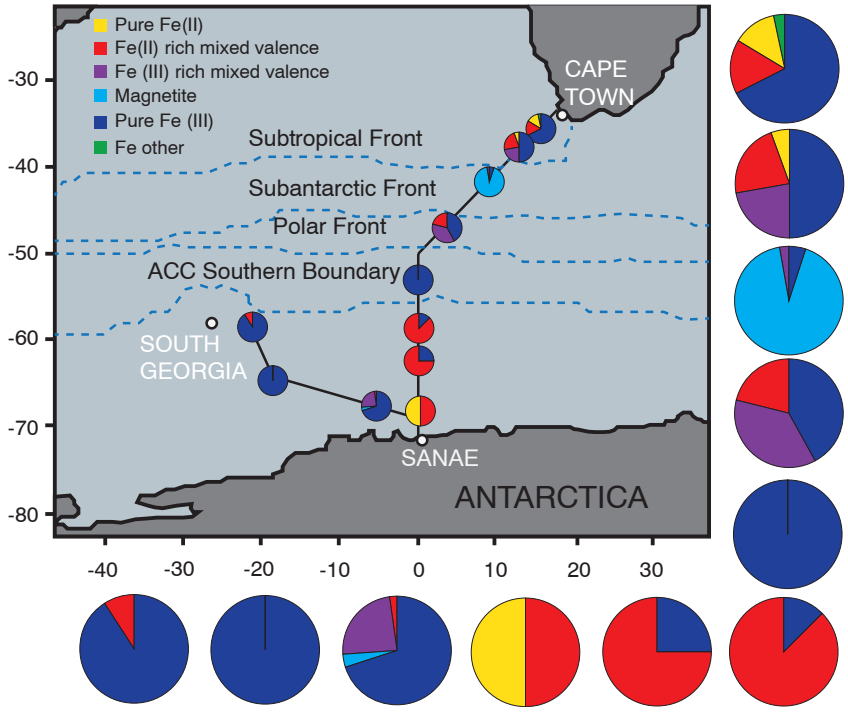

Fig. 3. Surface water transects (SANAE 49 and SANAE 50) of the South Atlantic and Southern oceans, and Fe speciation along the cruise transects. Sampling was conducted at different locations on these transects so as to ensure complete spatial resolution between the pertinent oceanic fronts. The pie charts (and their enlarged counterparts) show the relative contribution of Fe species, as defined by their spectral features, in the solid-phase Fe pool at each site. The Antarctic Circumpolar Current (ACC) Southern Boundary is defined as the southern terminus of the Upper Circumpolar Deep Water (*13*).

and additional x-ray spectroscopy measurements at the aluminum, silicon (~1840 eV), and carbon (~285 eV) edges show that these phases are not ferrous aluminosilicates and that they exhibit strong association with organic carbon. Possible contributors to the stability of these Fe(II) particles are the presence of thick organic coatings (or organic complexes) on their surfaces, photochemical reduction of Fe(III), structural impurities, and the slower oxidation rate of Fe(II) at low temperatures.

We also found Fe(III)-rich particles within the Southern Boundary front on the SANAE–South Georgia Island transect. The differences in Fe speciation between the two transects off the Antarctic shelf may be caused by differences in Fe sources, with westward samples likely displaying island effects from the upstream South Sandwich Island chain. Although not extensively examined, variable speciation with water column depth was observed on the basis of a single depth profile collected beyond the continental slope of southern Africa, suggesting internal recycling and possible differences in biological processing and Fe sources at different depths (fig. S2).

The association of Al [a well-known solubility modifier of Fe(III) minerals] with Fe in particles also showed variations along the two transects (Fig. 4). Aluminum substitution for Fe(III) in Fe oxides is commonly encountered in weathered material in the pedosphere, where Al/Fe ratios range between 0 and 0.47 for soil goethite (*15*) and amorphous phases often display higher values. We found that surface Fe particles collected nearer to and downstream of continental and island arc shelves, with the exception of the Antarctic shelf where Fe(II) phases predominate, typically exhibit relatively high Al/Fe ratios between 0.01 and 0.27. Off the African coast, the Al/Fe ratio increased with distance away from the fluvial source before dropping to lower values in the open ocean (Fig. 4). The Antarctic shelf showed predominantly Fe(II)-rich phases whose Al/Fe ratios were low or undetectable because of limited substitution of Al for Fe(II). Where depth samples were analyzed, the Al/Fe ratios were much higher (~0.17) at depth relative to the corresponding surface values (~0.08)—possibly a consequence of the solubility-depressing effect of Al substitution on sinking Fe particles, which would preserve only the most recalcitrant Al-rich phases from mineralization.

Laboratory studies have indicated that the biological availability of Fe is strongly linked to its solubility, which is influenced by chemical speciation [Fe(II) is more soluble (e.g., south of the Southern Boundary)], mineralogy (amorphous phases are more soluble), and Al substitution in Fe(III) oxides [Al-rich Fe phases are less soluble (e.g., the subtropical domain)]. Because all of these Fe forms exist in different abundances in different parts of the Southern Ocean, variation in the bioavailability of the Fe pool should be influenced by these factors. In addition, heterogeneity in the surface chemistry of the different Fe particles found in the water column is expected to affect the ability of microorganisms to scavenge Fe and other essential trace elements such as Cu and Zn, which are strongly associated with the Fe particle surfaces (*16*).

Sustained primary productivity requires the constant replenishment of the truly dissolved bioavailable Fe pool, which is continually being used by ambient phytoplankton species. One mechanism for this replenishment is by dissolution of the solid-phase Fe pool. Given that Fe solubility for the relatively simple Fe oxide and oxyhydroxide system varies over three orders of magnitude (*8*), our findings on heterogeneity in Fe particle chemistry imply that the solubility and expected dissolution rates of Fe particles vary regionally in the Southern Ocean. The causes of the observed heterogeneity in Fe speciation and its implications for Fe bioavailability are uncertain. However, a comparison between the average summertime chlorophyll a concentration and the abundance and distribution of labile Fe forms [for example, Fe(II)] reveals trends (*5*) (figs. S3 to S5) that allude to the effect of Fe speciation on biology, and vice versa.

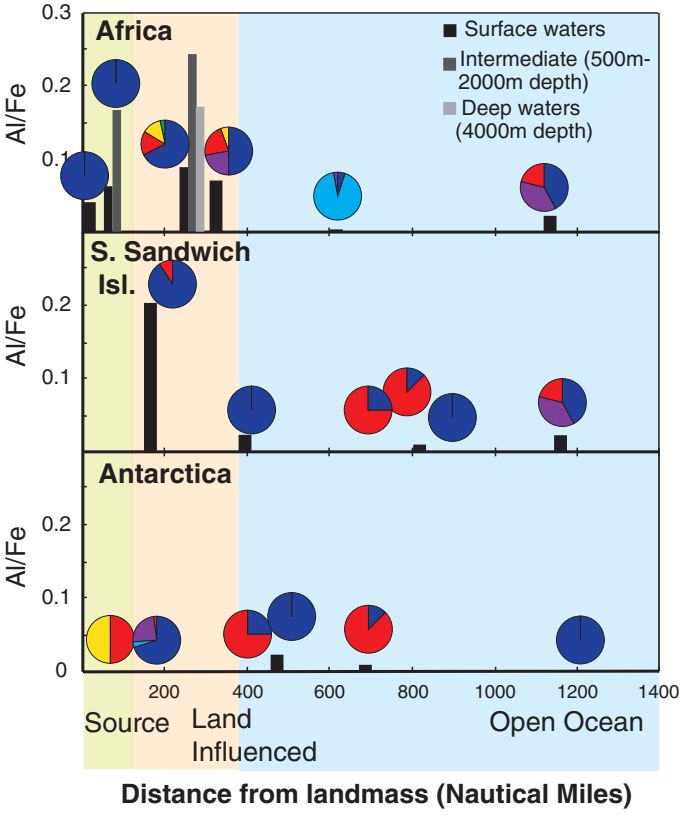

Fig. 4. Variations in the Al/Fe ratio of Fe particles with increasing distance from land mass and with depth. Source regions include fluvial inputs from the African river systems described in the text as well as marine sites located on the respective continental shelves. Land-influenced sites, which typically show higher Al/Fe ratios, are potentially influenced by continental and shelf sources. They are designated taking into account the vectors of ocean current movement and are all located within distances previously reported for continental Fe supply (*17*). Iron speciation pie charts are included to match the Al/Fe data to the sampling sites shown in Fig. 3.

References and Notes

1. P. W. Boyd, M. J. Ellwood, *Nat. Geosci.* **3**, 675 (2010).
2. W. G. Sunda, in *The Biogeochemistry of Iron in Seawater*, D. R. Turner, K. A. Hunter, Eds. (Wiley, New York, 2001), pp. 41–84.
3. F. Chever *et al.*, *J. Geophys. Res.* **115**, C10059 (2010).
4. J. Nishioka *et al.*, *Mar. Chem.* **95**, 51 (2005).
5. See supplementary materials on *Science* Online.
6. R. M. Cornell, U. Schwertmann, *The Iron Oxides: Structure, Properties, Reactions, Occurrences and Uses* (VCH, Weinheim, Germany, 2003).
7. M. Oakes, R. J. Weber, B. Lai, A. Russell, E. D. Ingall, *Atmos. Chem. Phys.* **12**, 745 (2012).
8. S. M. Kraemer, *Aquat. Sci.* **66**, 3 (2004).
9. H. Bluhm *et al.*, *J. Electron Spectrosc. Relat. Phenom.* **150**, 86 (2006).
10. G. van der Laan, I. W. Kirkman, *J. Phys. Condens. Matter* **4**, 4189 (1992).
11. F. M. F. de Groot, *J. Phys. Conf. Ser.* **190**, 012004 (2009).
12. N. Cassar *et al.*, *Science* **317**, 1067 (2007).
13. R. T. Pollard, M. I. Lucas, J. F. Read, *Deep Sea Res. II* **49**, 3289 (2002).
14. R. F. Anderson *et al.*, *Science* **323**, 1443 (2009).
15. R. W. Fitzpatrick, U. Schwertmann, *Geoderma* **27**, 335 (1982).
16. L. Balistrieri, J. W. Murray, *Geochim. Cosmochim. Acta* **47**, 1091 (1983).
17. P. J. Lam *et al.*, *Global Biogeochem. Cycles* **20**, GB1006 (2006).

Acknowledgments: Supported by grants from National Research Foundation, South Africa (Blue Skies Program and SANAP), Stellenbosch University VR(R) fund, NSF (chemical sciences), the U.S. Department of Energy (Office of Basic Energy Sciences and Subsurface Biogeochemical Research program), and the Princeton in Africa program. We thank the support staff at the Advanced Light Source for helping with data collection and sample preparation. This work benefited from discussions with F. Morel, D. Sigman, and four anonymous reviewers.

Supplementary Materials

www.sciencemag.org/cgi/content/full/338/6111/1199/DC1
Materials and Methods
Supplementary Text
Figs. S1 to S5
Table S1
References (*18*–*53*)

16 July 2012; accepted 16 October 2012
10.1126/science.1227504

Chemically and Geographically Distinct Solid-Phase Iron Pools in the Southern Ocean

B. P. von der Heyden, A. N. Roychoudhury, T. N. Mtshali, T. Tyliszczak and S. C. B. Myneni

Science **338** (6111), 1199-1201.
DOI: 10.1126/science.1227504

Swimming in Iron Pools

Because iron is essential for marine phytoplankton growth, its availability limits the primary productivity of the oceans. Iron is typically bioavailable only when present in a dissolved state; however, a large fraction of the total iron in the oceans exists as tiny solid-phase particles ranging in size from a few nanometers to a few micrometers. **von der Heyden *et al.*** (p. 1199) used high-resolution x-ray microscopy and spectroscopy to characterize the distribution of iron particles along two transects of the Southern Ocean. Analysis of a number of individual particles reveals strong variation in iron oxidation state, particle mineralogy, and substitution of aluminum for iron—all of which control the solubility, and hence bioavailability, of iron.